



# A Methodology for Measuring Selected Performance Parameters of Smartphone-Based Vehicle-to-Pedestrian and Pedestrian-to-Infrastructure Communication

Tibor Petrov<sup>(✉)</sup> 

Department of International Research Projects – ERAdiate+, University of Zilina, Univerzitna 8215/1, 010 26 Zilina, Slovakia  
tibor.petrov@uniza.sk

**Abstract.** Cooperative Intelligent Transport Systems (C-ITS) promise to bring large benefits in terms of increased transport safety. While some communication technologies used in C-ITS, such as Dedicated Short-Range Communications, have been already available for a long time, they were never adopted on a mass scale in consumer electronics, severely limiting the options for Vulnerable Road Users (VRUs) to foster the benefits of C-ITS. This situation might change with the advent of 5G-enabled smartphones. However, thorough testing of the available 5G networks is necessary before the deployment of C-ITS services to ensure their reliable operation. In this paper, we present a methodology for measuring and evaluating the selected performance parameters of V2P and Pedestrian-to-Infrastructure (P2I) communication based on 5G Uu communication interface using off-the-shelf hardware likely to be used by VRUs. We present a set of mobile applications that emulate V2P and P2I message transmissions and measure the increase in communication delay and message loss. Furthermore, we demonstrate the methodology of data collection and evaluation on a real case study conducted in the city of Zilina, Slovakia. The results suggest that the currently deployed commercial 5G networks can support V2P communication over Uu interface reliably if the generation frequency of the communication messages remains low.

**Keywords:** Vulnerable Road Users · Intelligent Transport Systems · V2P · P2I · C-ITS · VRU protection services · 5G communication · 5G performance evaluation

## 1 Introduction

With the advent of information and communication technologies, many industries have been transformed. This is also the case in transportation, where Intelligent Transport Systems (ITS) have been progressively deployed over the last decades in order to improve traffic safety, efficiency and management [1].

A further step in the evolution of ITS came with the introduction of Cooperative ITS (C-ITS), a system where transport system entities, such as vehicles, pedestrians and roadside infrastructure exchange information and cooperate together to further increase the efficiency of reaching their common goal. Examples of C-ITS applications include, among others, cooperative maneuvering in order to avoid collision, cooperative navigation to reduce traffic congestion or green light optimal speed advisory to improve the traffic flow at signalized intersections [2–4]. Furthermore, all of the C-ITS entities can leverage the connectivity to the Internet in order to benefit from a variety of additional data and services, such as real-time weather information, road condition, traffic status and infotainment services, making them important elements of the Internet of Everything.

The most promising benefit of C-ITS deployment comes in terms of increased situational awareness of vehicles and their drivers, which is expected to increase road safety significantly [5–7]. While the road traffic accident numbers in Europe have been steadily decreasing over the past decade - a trend significantly supported by ever-increasing technological advances in the automotive industry, the number of pedestrian casualties resulting from traffic accidents remains relatively stable. For this reason, there have been considerable efforts by the industry and academia aimed at introducing C-ITS for pedestrian safety applications.

In [8], the authors investigate the feasibility of crash avoidance applications to protect pedestrians and propose an architecture for Vehicle-to-Pedestrian (V2P) crash avoidance systems using Dedicated Short-Range Communications (DSRC)-enabled smartphone. In [9], Anaya et al. propose a pedestrian protection application based on Wi-Fi communication which allows to quantify the risk of collision and issue hazard warnings to pedestrians in the case they are present in the geographical area where a collision may occur. Wu et al. [10] developed a collision avoidance system which utilizes DSRC-based V2P communication to warn both pedestrians and drivers about a potential collision. Similar as in [8], the authors assume presence of DSRC communication stack in a smartphone to enable V2P communication.

One of the main barriers preventing the abovementioned efforts from being fully taken advantage of so far was a lack of a suitable communication technology to enable bi-directional data exchange between vehicles, pedestrians and the roadside digital infrastructure. DSRC commonly used for Vehicle-to-Vehicle (V2V) and Vehicle-to-Infrastructure (V2I) communication has not been widely adopted by the consumer electronics industry, resulting in low availability of the necessary communication hardware and protocols in communication terminals commonly used by pedestrians, such as smartphones. These, instead, almost exclusively rely on now ubiquitous cellular communication infrastructure. However, until recently, many studies pointed out that cellular networks have not been able to provide the high reliability and low latency required for safety-related applications in road transport [11–13]. This is expected to change with the proliferation of 5G New Radio (NR) cellular technology with performance enhancements promising to accommodate, among others, ultra-reliable low latency communication for safety-related applications.

In [14] the authors propose a hardware and software architecture for a pedestrian collision detection system based on V2P communication. With the advent of reliable and low-latency cellular communications, such as the one provided by 5G NR technologies,

a similar architecture could be used for a pedestrian protection system relying on Cellular Vehicle-to-Everything (C-V2X) communication instead of the short-range Wi-Fi communication as proposed in the paper.

Widespread deployment of C-ITS services which may rely on communication network resources shared with other users and applications can impact the performance of other Internet of Everything applications. Therefore, to understand the impact of pedestrian protection C-ITS services on the performance of the communication network and ensure that these services can be reliably supported by the currently deployed 5G networks in their targeted deployment area, extensive data collection and service testing is necessary.

This paper presents a methodology for data collection and evaluation to identify potential performance limitations of currently deployed commercial 5G networks in the context of pedestrian communication and assess their potential to support V2P and Pedestrian-to-Infrastructure (P2I) communication applications relying on C-V2X communication using the Uu cellular communication interface. Application of the proposed methodology is demonstrated on a case study conducted in the part of the city of Zilina, Slovakia, in order to assess the ability of the commercial 5G network, currently deployed in the case study area, to fulfill the communication requirements of pedestrian protection C-ITS services.

The rest of the paper is organized as follows. Section 2 introduces the communication requirements of common C-ITS applications. In Sect. 3, the data collection and processing methodology is described. Section 4 illustrates the application of the proposed methodology on an example of a case study carried out in the part of the city of Zilina in Slovakia. Finally, Sect. 5 concludes the paper and discusses the identified limitations of the proposed methodology as well as the further steps necessary to address them.

## 2 Communication Requirements of C-ITS Applications

The general requirements for data exchange in the context of Vulnerable Road User (VRU) communication in Europe are set by the European Telecommunication Standards Institute (ETSI) in [15, 16]. The VRU basic service (VBS) defined therein can be used by various C-ITS applications which provide safety and value to the user. Table 1 provides examples of such C-ITS applications and their estimated communication requirements in terms of communication latency and required data rate. It is worth mentioning here, that data exchanges are carried out by Vulnerable Road User Awareness Messages (VAMs) disseminated with a variable length and message generation frequency. Therefore, the VBS has been designed to be flexible enough in order to support the communication requirements of many current and future C-ITS applications.

## 3 Methodology

The data collection for measuring the communication performance parameters is performed by a pair of Android mobile applications which we developed for the purpose. One of the applications, referred to as Sender Mobile App acts as a client generating network traffic with configurable parameters. The other application, referred to as Receiver

**Table 1.** Example of communication requirements of C-ITS applications for VRU protection.

Service	Latency	Data rate
VRU collision warning	$\leq 100$ ms	$\sim 100$ kbps
Blind spot VRU detection	$\leq 100$ ms	$\sim 50$ kbps
Vehicle turning warning	$\leq 100$ ms	$\sim 50$ kbps
VRU priority	$\leq 500$ ms	$\sim 50$ kbps
Data crowdsourcing for traffic management	$\leq 1000$ ms	$\geq 1$ Mbps

Mobile App acts as a server, listening for communications from the Sender Mobile App. These applications perform three main tasks. First, they facilitate end-to-end data exchange over a commercial mobile network between two Android devices. The communication is carried out utilizing the Uu interface, i.e. the radio interface between the smartphone and the cellular base station. Second, they collect data necessary for the computation of the communication KPIs. Third, they provide a minimalistic, simple-to-use User Interface (UI) to change the communication parameters and check the correct operation of the respective app. The screenshots from both apps, showcasing their controls and UI are presented in Fig. 1a and Fig. 1b.

### 3.1 Sender Mobile App

The Sender Mobile App generates communication messages with a predefined periodicity and length and sends them to a predefined IP address using UDP transport protocol.

Upon its launch, the application initializes Android's location service and asks the user for allowing necessary permissions in order to access the device's fine location returned by available Global Navigation Satellite Systems (GNSS).

The message generation frequency  $f_m$ , message length  $L_m$  and the destination IP address of the communication are user-configurable and can be changed during the application runtime. The  $L_m$  can be changed in the range from 10 to 1500 Bytes either using a seek bar Android widget, or by directly typing the desired length in Bytes to the editable text UI component, as can be seen in Fig. 1a. The  $f_m$  can be set in the range from 0.5 to 20 messages per second using another seek bar widget. The ranges for the  $L_m$  and  $f_m$  were selected so they are consistent with the expected range of message lengths and generation frequencies of ETSI VBS [15].

After the destination IP address is entered using another editable text UI component, the communication can be initiated by tapping the Start Service button. When the communication is initiated, a local log file is created on the device's internal storage. In this log, a sequence number of each sent message and the information about the serving cell base station at the time of sending the message is stored. Based on the data available from the serving base station, the cell information may include: the cell type (LTE or 5G NR), cell ID, tracking area code, used bands, cell signal strength, Received Signal Strength Indication (RSSI), Reference Signal Received Quality (RSRQ), Channel Quality Indicator (CQI).

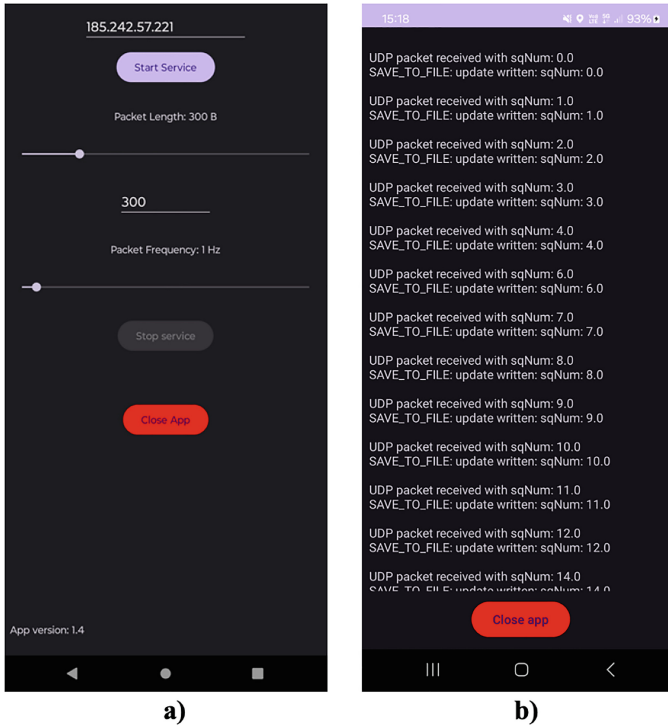


**Fig. 1.** User interface of the measuring apps: a) Sender Mobile App; b) Receiver Mobile App.

Upon initiating the communication by the user, the Sender Mobile App opens a UDP socket and schedules a repeating timer with a fixed period of  $1/f_m$  seconds.

### 3.2 Receiver Mobile App

The Receiver Mobile App listens at a pre-configured UDP port for incoming messages from the Sender Mobile App and stores the data collection logs on the device's internal storage.

The Receiver Mobile App's main screen contains a text view component notifying the user about each received message to enable a basic level of oversight and troubleshooting in case of loss of communication. The only other graphical component on the Receiver Mobile App's screen is a red button which closes the app and stores the data collection log to the device's internal storage upon touching it.

Upon receiving a communication message from the Sender Mobile App, the Receiver Mobile App captures a message reception timestamp, extracts the payload data from the message, calculates the message transmission end-to-end delay and stores the received data and calculated delay to the log. The data stored to the device's internal storage include received message's sequence number, sending timestamp, reception timestamp, payload length, end-to-end delay, generation frequency and sending device's position and GNSS location accuracy.

### 3.3 Data Processing

To process and visualize the data collected during the measurements, a set of automated scripts have been created in Python programming language.

First, the delay data are processed. In this step, the measured delays are first normalized, i.e. their values are transformed as follows:

$$d_i \rightarrow d_i - d_{min}, \quad (1)$$

where  $d_i$  is the  $i$ -th observation of delay and  $d_{min}$  is the minimum delay value observed during the measurement session. This step is necessary to counteract the effect of imperfect clock synchronization of the two measuring devices. Hence, the transformed value of  $d_i$  does not represent the absolute value of the communication end-to-end delay, but rather the relative increase in end-to-end delay observed during the measurement session compared to the data point with the lowest measured delay.

Second, the message loss data are processed. Here, the log is searched for missing messages or messages received out of order based on the stored sequence numbers. We consider any message received out of order as lost, as in the case of VBS, its payload is considered outdated after any subsequent message carrying the status information of the sender is successfully received.

Finally, the delay and message loss data are visualized on a map using the Folium Python library. Delay data points are plotted in colors ranging from blue to red, where blue corresponds to the lowest relative latency and red corresponds to the highest relative latency. In the case of message loss data, lost messages are indicated as a change in the color of the data point corresponding to the previous successfully received message. Lost messages are indicated by colors ranging from green to red, where green corresponds to one lost message and red corresponds to the highest number of consecutive lost messages. Data points where no message loss has been experienced are plotted in blue.

Data visualization approach described here allows to quickly identify the most troublesome areas in terms of poor delay and message delivery performance in the measurement area.

## 4 Data Collection Example – Zilina Case Study

In this section, we demonstrate the use of the developed applications and the data processing methodology on a case study carried out in the part of the city of Zilina in the northwestern part of Slovakia.

First, using data from the traffic survey carried out for the city of Zilina's transport general plan, we identified the street with the highest volume of pedestrians where car traffic is also present. We selected this street as the target area for carrying out the measurements. The layout of the street presents a challenge, due to the canopies above the sidewalks, and high-rise apartment buildings, which may obstruct GNSS and cellular network signals, as can be seen in Fig. 2. The measurement area has been extended to cover also street around the city park with dense vegetation. The whole case study area is depicted in Fig. 3.



**Fig. 2.** Picture of the part of the measurement area. Canopies sheltering part of the sidewalks on both sides of the street challenge the reception of GNSS and cellular network signals.

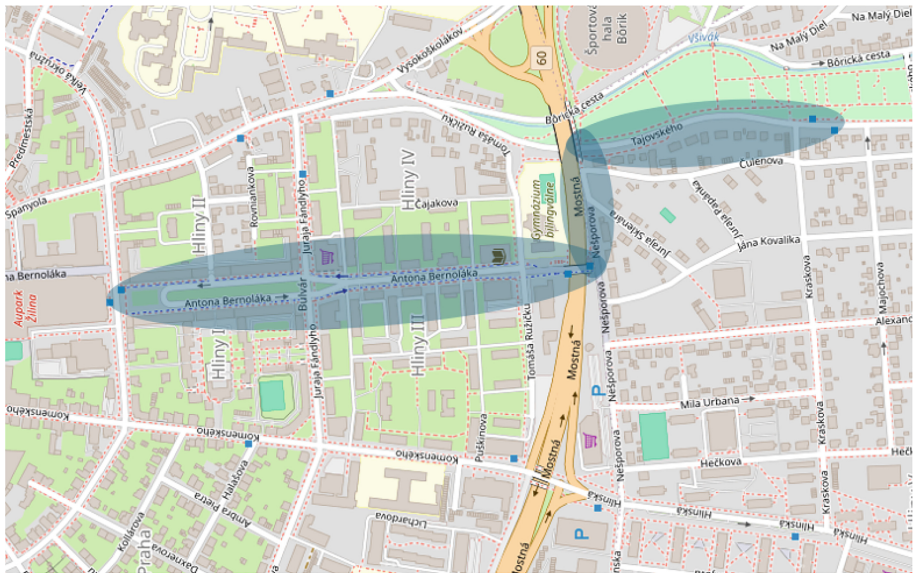


**Fig. 3.** Location of the case study area.

The measurements were taken using two 5G-enabled Android smartphones using the same network provider. One device served as a communication client running the Sender Mobile App. The second device served as a communication server running the Receiver Mobile App. Both devices moved along the same trajectory with the same velocity and were located in close proximity of each other.

Between the measuring sessions, we varied message length  $L_m$  (300 Bytes and 1500 Bytes) and message generation frequency  $f_m$  (1 Hz and 10 Hz). Both  $L_m$  and  $f_m$  were kept

constant within a single measuring session. In total, four combinations of communication parameters were considered and average values of two measuring sessions, conducted in different times and days are showcased in this paper. In total, eight measuring sessions were conducted. Based on the measured data, we evaluated the relative increase in communication end-to-end delay  $\Delta d$ , average message loss ratio (*MLR*) and the number of consecutive lost messages  $N_{lost}$  between two successfully delivered messages.

The results in terms of  $\Delta d$  are visualized in Fig. 4. The average value of  $\Delta d$ , i.e.,  $\Delta d_{avg}$ , observed when transmitting messages with  $L_m$  of 300 Bytes with  $f_m$  of 1 Hz (Fig. 4a) is  $(0.02 \pm 0.01)$  ms and the maximum value of  $\Delta d$ , i.e.,  $\Delta d_{max}$ , reached just 0.21 ms. In the case of messages generated with the same frequency, but with a larger  $L_m$  of 1500 Bytes (Fig. 4c), the value of  $\Delta d_{avg}$  is just slightly larger, i.e.,  $(0.03 \pm 0.05)$  ms and  $\Delta d_{max}$ , in this case, reached 1.54 ms. This indicates that the end-to-end delay of the message transmissions is rather stable throughout the measurement sessions and does not grow significantly with the increase of  $L_m$ .

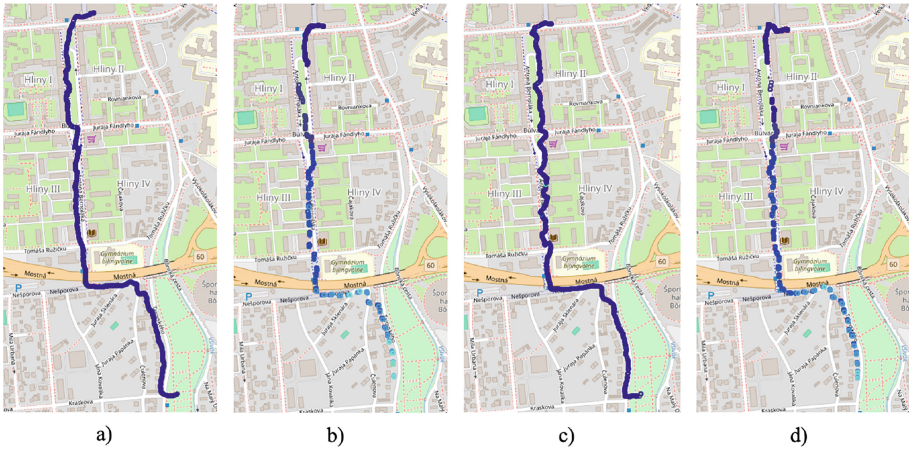


**Fig. 4.** Relative increase in communication end-to-end delay  $\Delta d$  measured using different values of message length  $L_m$  and message generation frequency  $f_m$ : a)  $L_m = 300B, f_m = 1$  Hz; b)  $L_m = 300B, f_m = 10$  Hz; c)  $L_m = 1500B, f_m = 1$  Hz; d)  $L_m = 1500B, f_m = 10$  Hz.

In the case of 10 Hz  $f_m$ , the observed  $\Delta d_{avg}$  is  $(24.67 \pm 19.39)$  ms and  $(24.37 \pm 20.83)$  ms for  $L_m$  of 300 Bytes (Fig. 4b) and 1500 Bytes (Fig. 4d) respectively. The value of  $\Delta d_{max}$  reached 74.25 ms for  $L_m$  of 300 Bytes and 168.24 ms for  $L_m$  of 1500 Bytes. These results indicate that the  $f_m$  seems to have a larger impact on the  $\Delta d$  than  $L_m$ .

The average and maximum values of  $\Delta d$  observed for each combination of  $L_m$  and  $f_m$  are summarized in Table 2.

**Table 2.** Average and maximum values of increase in communication end-to-end delay.

Message length $L_m$ and message generation frequency $f_m$ values	Average increase in end-to-end delay $\Delta d_{avg}$ and the standard deviation	Maximum increase in end-to-end delay $\Delta d_{max}$
$L_m = 300B, f_m = 1$ Hz	(0.02 $\pm$ 0.01) ms	0.21 ms
$L_m = 300B, f_m = 10$ Hz	(24.67 $\pm$ 19.39) ms	74.25 ms
$L_m = 1500B, f_m = 1$ Hz	(0.03 $\pm$ 0.05) ms	1.54 ms
$L_m = 1500B, f_m = 10$ Hz	(24.37 $\pm$ 20.83) ms	168.24 ms

The communication reliability in terms of average MLR and the maximum  $N_{lost}$  for each investigated combination of communication parameters is summarized in Table 3 and the latter is also visualized in Fig. 5. The results indicate that the MLR tends to decrease slightly as the message length increases. This decrease in MLR is more pronounced for  $f_m$  of 1 Hz and demonstrates only slightly for  $f_m$  of 10 Hz.

**Table 3.** Average message loss ratio and maximum number of consecutive lost messages.

Message length $L_m$ and message generation frequency $f_m$ values	Average message loss ratio	Maximum number of consecutive lost messages
$L_m = 300B, f_m = 1$ Hz	7.3%	1
$L_m = 300B, f_m = 10$ Hz	64.8%	149
$L_m = 1500B, f_m = 1$ Hz	0%	0
$L_m = 1500B, f_m = 10$ Hz	63.9%	139

Furthermore, the MLR increases dramatically with the increase of the  $f_m$  from 1 Hz to 10 Hz from up to 7.3% to more than 63% for both investigated values of message length  $L_m$ . This again indicates that the performance of the investigated commercial 5G network is optimized more toward supporting the transmission of large, low-frequency messages. This is a challenge for safety-related C-ITS message transmissions, as those tend to rely on shorter messages which are transmitted rather frequently to ensure the recipient application works with the up-to-date status information.

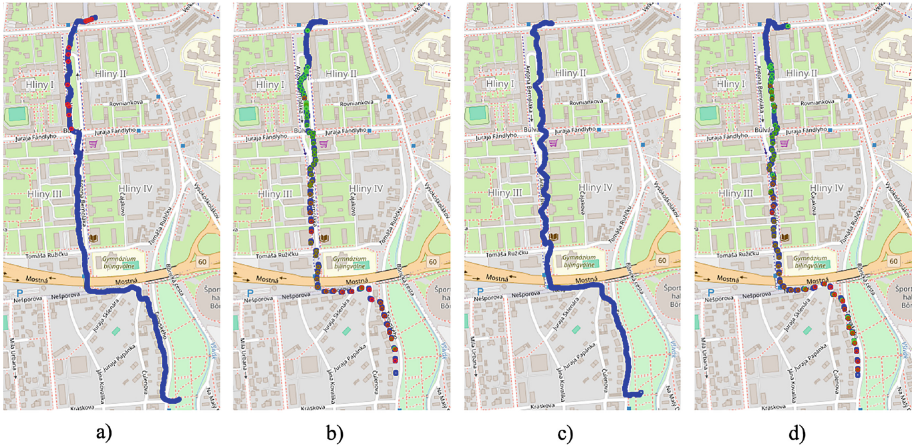


**Fig. 5.** Message loss measurements taken using different values of message length  $L_m$  and message generation frequency  $f_m$ : a)  $L_m = 300B$ ,  $f_m = 1$  Hz; b)  $L_m = 300B$ ,  $f_m = 10$  Hz; c)  $L_m = 1500B$ ,  $f_m = 1$  Hz; d)  $L_m = 1500B$ ,  $f_m = 10$  Hz.

## 5 Discussion and Conclusions

In this paper, we presented a methodology for measuring the key performance metrics of commercial 5G networks using a set of mobile applications which can emulate V2P and P2I communication using Uu cellular interface. Furthermore, we demonstrate the application of the methodology by conducting a performance evaluation of a commercial 5G network in the part of the city of Zilina, Slovakia.

The results of the performance evaluation suggest, that the currently deployed commercial 5G network can support V2P communication over Uu interface very reliably if the frequency of the communication messages remains low. In the case of one message being transmitted every second, the message loss ratio between 0 and 7.3% has been achieved with a negligible increase in the communication end-to-end delay.

However, in the case of frequent generation of communication messages, the network struggled to deliver messages reliably, reaching a very high message loss ratio of up to 64.8% for 10 Hz message generation frequency and a considerable increase of the communication end-to-end delay. Furthermore, the communication messages were lost in frequent bursts of up to 149 consecutive lost messages, which resulted in a loss of status information for the message recipient for prolonged periods of time. This indicates that the deployed 5G network in the case study area is currently not suitable for supporting high-frequency, low-latency V2P safety communications.

While the measuring applications presented herein are able to provide a sense of how communication end-to-end latency changes during a measurement session, they are currently unable to provide the absolute value of the end-to-end latency. This is caused by the difficulty of maintaining the sufficient level of accuracy in terms of clock synchronization of the two measurement devices.

In our future work, we will continue to enhance the accuracy of the data collection applications, especially in terms of measuring the actual value of communication end-to-end latency by using the very precise GNSS timings to synchronize the clock of the measurement devices in periodic time intervals. Solving this issue will enable the possibility of evaluating the measurements in real time, further increasing the practical utility of the developed tools and methods in terms of enabling a quick and low-cost evaluation of the communication performance in any segment of road infrastructure. Furthermore, additional data collection and research is needed to understand the impact of the deployment of C-ITS services over a cellular network on the performance of other Internet of Everything applications.

**Acknowledgments.** This work was supported by the Grant System of the University of Žilina under project ID 18730 “Utilization of commercial 5G networks for supporting services based on Vehicle to Infrastructure to VRU communication”.

## References

1. Auer, A., Feese, S., Lockwood, S., Hamilton, B.A.: History of intelligent transportation systems. United States Department of Transportation Intelligent Transportation Systems Joint Program Office Technical Report (No. FHWA-JPO-16-329) (2016)
2. Hameed Mir, Z., Filali, F.: C-ITS applications, use cases and requirements for V2X communication systems—threading through IEEE 802.11 p to 5G. In: Pathan, A.S.K. (ed.) *Towards a Wireless Connected World: Achievements and New Technologies*, pp. 261–285. Springer, Heidelberg (2022). [https://doi.org/10.1007/978-3-031-04321-5\\_11](https://doi.org/10.1007/978-3-031-04321-5_11)
3. Biral, F., Valenti, G., Bertolazzi, E., Steccanella, A.: Cooperative safety applications for C-ITS equipped and non-equipped vehicles supported by an extended local dynamic map built on safe strip technology. In: 2019 15th International Conference on Distributed Computing in Sensor Systems (DCOSS), pp. 733–740. IEEE, New York (2019)
4. Mellegård, N., Reichenberg, F.: The day 1 C-ITS application green light optimal speed advisory—a mapping study. *Transp. Res. Procedia* **49**, 170–182 (2020)
5. Javed, M.A., Hamida, E.B.: Measuring safety awareness in cooperative ITS applications. In: 2016 IEEE Wireless Communications and Networking Conference, pp. 1–7. IEEE, New York (2016)
6. Vorobyev, A.I., Pletnev, M.G., Koveshnikov, A.A., Vorobyeva, T.V., Morozov, D.Y.: Providing additional situational awareness with the use of V2X technology to improve the reliability of highly automated vehicles. In: 2021 Systems of Signals Generating and Processing in the Field of on Board Communications, pp. 1–4. IEEE, New York (2021)
7. Kang, J., Tak, S., Park, S.: Analyzing the impact of C-ITS services on driving behavior: a case study of the Daejeon-Sejong C-ITS pilot project in South Korea. *Sustainability* **15**(16), 12655 (2023)
8. Tahmasbi-Sarvestani, A., Kazemi, H., Fallah, Y.P., Naserian, M., Lewis, A.: System architecture for cooperative vehicle-pedestrian safety applications using DSRC communication. SAE Technical Paper (No. 2015-01-0290) (2015)
9. Anaya, J.J., Merdrignac, P., Shagdar, O., Nashashibi, F., Naranjo, J.E.: Vehicle to pedestrian communications for protection of vulnerable road users. In: 2014 IEEE Intelligent Vehicles Symposium Proceedings, pp. 1037–1042. IEEE, New York (2014)

10. Wu, X., et al.: Cars talk to phones: a DSRC based vehicle-pedestrian safety system. In: 2014 IEEE 80th Vehicular Technology Conference (VTC2014-Fall), pp. 1–7. IEEE, New York (2014)
11. Karoui, M., Freitas, A., Chalhoub, G.: Performance comparison between LTE-V2X and ITS-G5 under realistic urban scenarios. In: 2020 IEEE 91st Vehicular Technology Conference (VTC2020-Spring), pp. 1–7. IEEE, New York (2020)
12. Luoto, P., Bennis, M., Pirinen, P., Samarakoon, S., Horneman, K., Latva-Aho, M.: System level performance evaluation of LTE-V2X network. In: European Wireless 2016, 22th European Wireless Conference, pp. 1–5. VDE, Berlin (2016)
13. Shi, M., Lu, C., Zhang, Y., Yao, D.: DSRC and LTE-V communication performance evaluation and improvement based on typical V2X application at intersection. In: 2017 Chinese Automation Congress (CAC), pp. 556–561. IEEE, New York (2017)
14. Arena, F., Pau, G., Severino, A.: V2X communications applied to safety of pedestrians and vehicles. *J. Sens. Actuator Netw.* **9**(1), 3 (2019)
15. ETSI TS 103 300-2 v2.1.1. [https://www.etsi.org/deliver/etsi\\_ts/103300\\_103399/10330002/02.01.01\\_60/ts\\_10330002v020101p.pdf](https://www.etsi.org/deliver/etsi_ts/103300_103399/10330002/02.01.01_60/ts_10330002v020101p.pdf). Accessed 5 June 2024
16. ETSI TS 103 300-3 v2.1.1. [https://www.etsi.org/deliver/etsi\\_ts/103300\\_103399/10330003/02.01.01\\_60/ts\\_10330003v020101p.pdf](https://www.etsi.org/deliver/etsi_ts/103300_103399/10330003/02.01.01_60/ts_10330003v020101p.pdf). Accessed 5 June 2024